Electronic Supplementary Information for

Fluorescence Enhancement in Crystals Tuned by a Molecular Torsion Angle: A Model to Analyze Structural Impact

P. Srujana, Tarun Gera and T. P. Radhakrishnan*
School of Chemistry, University of Hyderabad
Hyderabad – 500 046, India

Contents **Page**

Synthesis and Characterization

Synthesis was carried out following Route B in Fig. 1 (main text) [Fig. S1 (page S3)].

7-pyrrolidino-7,8,8-tricyanoquinodimethane (PTCNQ)

The procedure reported in Ref. 14 (main text) was followed with minor modifications. Pyrrolidine (0.095 ml, 1.136 mmol) was added to a warm solution of TCNQ (0.29 g, 1.4 mmol) in 35 ml acetonitrile; the solution turned dark green immediately and then changed to dark purple (CAUTION: small amount of HCN gas is formed as the byproduct of the reaction, but possibly remains dissolved in the solution). It was stirred at 65°C for 4 h and then cooled to 4°C. The microcrystalline solid which precipitated over 2 days was filtered, washed with acetonitrile and dried to give PTCNQ (0.23 g, 82% yield).

2-(4-dicyanomethylenecyclohexa-2,5-dieny1idene)-imidazolidine (1a)

Ethylenediamine (0.054 ml, 0.806 mmol) was added to a warm solution of PTCNQ (0.2 g, 0.806 mmol) in 25 ml acetonitrile. The solution turned dark green immediately and a microcrystalline solid precipitated. It was stirred for 4 h at 70°C and cooled to room temperature (~ 25°C). The microcrystalline solid was filtered, washed with acetonitrile and dried to give **1a** (0.19 g, 79% yield). The compound was dissolved in dimethylformamide and cooled to 4°C. Crystallization was induced by diffusion of diethyl ether; crystals grown in the solution over four days were filtered out. mp: 280°C (from DMF, dec.); FTIR (KBr) - $\bar{\upsilon}$/cm^{-1}: 3199(broad, NH), 2191.7 (CN), 2147.8 (CN), 1605.4 and 1506.8 (Ar ring C-C); NMR (400 MHz, DMSO-d_6) - δ/ppm ^{1}H: 9.77 (s, 2H, 2NH), 7.59-7.57 (d, 2H, 2 aromatic CH), 6.84-6.82 (d, 2H, 2 aromatic CH), 3.89 (s, 4H, 2CH_2); ^{13}C: 164.62, 150.43, 129.38, 123.31, 117.81, 108.6, 44.25, 35.34; HRMS (ESI) - *m*/*z*: 210.0905 (calculated for $C_{12}H_{10}N_4$ [M^+]: 210.0905).

2-(4-dicyanomethylenecyclohexa-2,5-dieny1idene)-1-ethylimidazolidine (1b)

N-ethylethylenediamine (0.103 ml, 0.806 mmol) was added to a warm solution of PTCNQ (0.2 g, 0.806 mmol) in 25 ml acetonitrile. The solution turned dark green immediately and turned reddish orange in ~ 30 min. It was stirred for 4 h at 70°C and cooled to ambient temperature (~25°C). The microcrystalline solid which precipitated over 6 days was filtered, washed with acetonitrile and dried to give **1b** (0.16 g, 82% yield). mp: 255-258°C (from MeCN, dec.); FTIR (KBr) - $\bar{\upsilon}$/cm^{-1}: 3545(broad, OH), 3150.2 (NH), 2186.2 (CN), 2136.9 (CN), 1583.5 and 1512.3 (Ar ring C-C), 1331.5 (CH); NMR (400 MHz, DMSO-d_6) - δ/ppm ^{1}H: 9.71 (s, 1H, 1NH) 7.31-7.29 (d, 2H, 2 aromatic CH), 6.88-6.86 (d, 2H, 2 aromatic CH), 4.02-3.96 (t, 2H, CH_2), 3.85-3.83 (t, 2H, CH_2), 3.51-3.49 (q, 2H, CH_2), 1.25 (t, 3H, CH_3); ^{13}C: 166.18, 149.29, 129.67, 123.77, 117.97, 109.16, 49.70, 42.91, 42.20, 33.77, 13.19; HRMS (ESI) - *m*/*z*: 239.1294 (calculated for $C_{14}H_{15}N_4$ [M^++H]: 239.1297).

2-(4-dicyanomethylenecyclohexa-2,5-dieny1idene)-1,3-dimethylimidazolidine (1c)

N,N'-dimethylethylenediamine (0.103 ml, 0.806 mmol) was added to a warm solution of PTCNQ (0.2 g, 0.806 mmol) in 25 ml acetonitrile. The solution turned dark green immediately and turned reddish orange in ~ 30 min. It was stirred for 4 h at 70°C and cooled to ambient temperature (~25°C). The crystalline solid which precipitated over 8 days was filtered, washed with acetonitrile and dried to give **1c** (0.12 g, 63% yield). mp: 327-331°C (from MeCN); FTIR (KBr) - $\bar{\upsilon}$/cm^{-1}: 2936.9 (weak, Ar CH), 2175.3 (CN), 2131.4 (CN), 1594.5 and 1501.3 (Ar ring

C-C), 1331.5 (CH); NMR (400 MHz, DMSO-d_6) - δ/ppm ^{1}H: 7.22-7.20 (d, 2H, 2 aromatic CH), 6.91-6.89 (d, 2H, 2 aromatic CH), 3.92 (s, 4H, $2CH_2$), 2.98 (s, 6H, $2CH_3$); ^{13}C: 166.32, 148.34, 130.02, 124.02, 118.01, 107.78, 50.20, 35.46, 32.96; HRMS (ESI) - *m*/*z*: 239.1296 (calculated for $C_{14}H_{15}N_4$ [M^++H]: 239.1297).

Possible routes for the synthesis of **1a** from TCNQ are shown in Fig. S1. In the original paper that reported **1a** (Ref. 14), synthesis was carried out using Route A, and the only characterizations provided were elemental analysis and ir spectrum. These would be consistent with either the monomer or oligomer structure shown along Route A. It was also mentioned in Ref. 14, that the compound did not melt till 405^{o}C; this could be indicative of a polymeric structure. **1a** that we have synthesized and structurally characterized is found to decompose irreversibly at 280^{o}C.

Figure S1. Scheme for the synthesis of **1a** from TCNQ following two routes; possible formation of polymeric products is indicated.

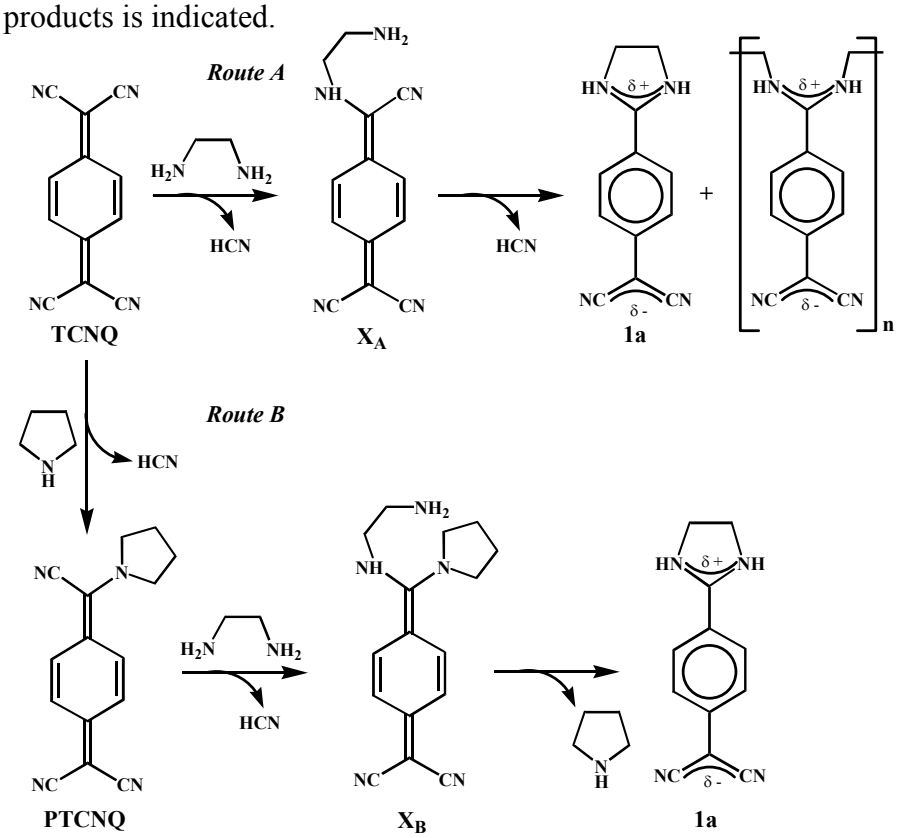

The reduced probability of polymeric product formation in Route B may be attributed to the following. The C atom bearing the cyano group in the intermediate X_A is relatively more electron poor than the corresponding C in X_B bearing a pyrrolidine group; hence the efficiency of nucleophilic attack of the amine on the C atom is enhanced in the former. Even though this would make the intramolecular cyclization more efficient in X_A, it will also facilitate intermolecular reactions as the entropy cost is partly offset by the high enthalpy gain. In the case of X_B, the intramolecular reaction is possibly slower, but at the same time, the intermolecular reaction becomes highly unlikely. Thus polymerization is possible along Route A, but not along Route B.

Crystal structure Details

Single crystal X-ray diffraction studies were carried out on a Bruker SMART APEX CCD area detector system equipped with a graphite monochromator and a MoK_α fine-focus sealed tube (λ = 0.71073 Å) operated at 1200 W (40 kV, 30 mA). Data was collected at 100 K, and the reduction was performed using Bruker SAINT software; the structure was solved and refined using the Bruker SHELXTL (Version 6.14) Software.

The molecular structure and unit cell packing from crystal structure determination, as well as the basic crystallographic information for **1a-c** are provided in the following pages.

CCDC deposition number for the three crystals:

1a **:** 1444520

1b **:** 1444521

1c **:** 1444522

Figure S2. Molecular structure showing 99% thermal ellipsoids and the unit cell of **1a**

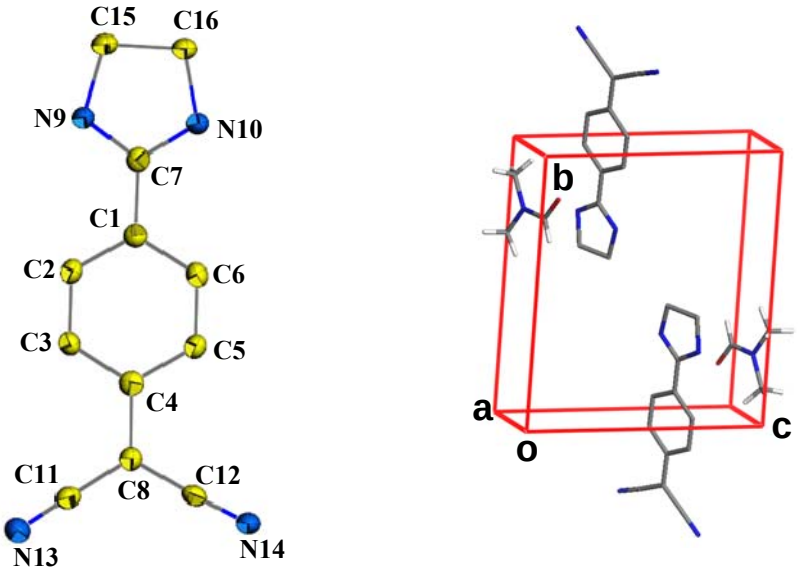

Table S1. Crystallographic details of **1a**

Common name	2-(4-dicyanomethylenecyclohexa-2,5-dieny1idene)-imidazolidine. DMF
Empirical formula	$C_{15}H_{17}N_5O$
Crystal system	Triclinic
Space group	P-*1*
a / Å	5.6328(5)
b / Å	11.2617(10)
c / Å	11.2686(10)
α / deg.	86.4430(10)
β / deg.	77.4390(10)
γ /deg.	85.4860(10)
V / $Å^3$	694.81(11)
Z	2
$\rho_{calc.}$ / g cm^{-3}	1.354
μ / cm^{-1}	0.09
Temperature / K	100(2)
λ / Å	0.71073
No. of reflections	2813
No. of parameters	258
Max., Min. transmission	0.964, 0.991
GOF	1.047
R [for $I \geq 2\sigma_I$]	0.0360
wR^2	0.10
Largest difference peak and hole / e$Å^{-3}$	0.239, 0.048

Table S2. Bond lengths and bond angles for **1a**

Atoms	Bond length (Å)	Atoms	Bond angle (°)	Atoms	Bond angle (°)
O(17)-C(18)	1.2383(14)	C(7)-N(10)-C(16)	111.29(9)	N(9)-C(15)-C(16)	102.59(8)
N(10)-C(7)	1.3284(13)	C(7)-N(10)-H(10)	124.4(9)	N(9)-C(15)-H(15A)	109.3(8)
N(10)-C(16)	1.4673(13)	C(16)-N(10)-H(10)	122.7(9)	C(16)-C(15)-H(15A)	111.0(8)
N(10)-H(10)	0.909(16)	C(18)-N(20)-C(21)	121.09(9)	N(9)-C(15)-H(15B)	109.6(8)
N(20)-C(18)	1.3276(14)	C(18)-N(20)-C(22)	121.18(9)	C(16)-C(15)-H(15B)	112.7(8)
N(20)-C(21)	1.4549(14)	C(21)-N(20)-C(22)	117.57(9)	H(15A)-C(15)-H(15B)	111.3(11)
N(20)-C(22)	1.4557(14)	C(7)-N(9)-C(15)	111.50(9)	N(9)-C(7)-N(10)	111.16(9)
N(9)-C(7)	1.3183(13)	C(7)-N(9)-H(9)	126.2(10)	N(9)-C(7)-C(1)	125.41(9)
N(9)-C(15)	1.4661(13)	C(15)-N(9)-H(9)	121.3(10)	N(10)-C(7)-C(1)	123.42(9)
N(9)-H(9)	0.944(17)	C(2)-C(3)-C(4)	121.20(9)	C(6)-C(5)-C(4)	121.06(10)
C(3)-C(2)	1.3803(14)	C(2)-C(3)-H(3)	120.0(8)	C(6)-C(5)-H(5)	120.4(8)
C(3)-C(4)	1.4089(14)	C(4)-C(3)-H(3)	118.8(8)	C(4)-C(5)-H(5)	118.5(8)
C(3)-H(3)	0.976(13)	N(14)-C(12)-C(8)	176.87(11)	N(20)-C(22)-H(22A)	109.2(8)
N(14)-C(12)	1.1598(14)	C(5)-C(6)-C(1)	121.17(10)	N(20)-C(22)-H(22B)	109.1(8)
C(12)-C(8)	1.4024(15)	C(5)-C(6)-H(6)	118.2(8)	H(22A)-C(22)-H(22B)	110.4(11)
N(13)-C(11)	1.1578(14)	C(1)-C(6)-H(6)	120.6(8)	N(20)-C(22)-H(22C)	109.4(8)
C(6)-C(5)	1.3741(15)	N(13)-C(11)-C(8)	178.85(11)	H(22A)-C(22)-H(22C)	109.3(11)
C(6)-C(1)	1.3991(14)	C(3)-C(2)-C(1)	120.70(9)	H(22B)-C(22)-H(22C)	109.4(11)
C(6)-H(6)	0.974(14)	C(3)-C(2)-H(2)	119.4(8)	N(10)-C(16)-C(15)	102.23(8)
C(11)-C(8)	1.4116(14)	C(1)-C(2)-H(2)	119.9(8)	N(10)-C(16)-H(16A)	110.0(8)
C(2)-C(1)	1.4042(14)	C(6)-C(1)-C(2)	118.34(9)	C(15)-C(16)-H(16A)	111.2(8)
C(2)-H(2)	0.940(15)	C(6)-C(1)-C(7)	120.37(9)	N(10)-C(16)-H(16B)	109.9(7)
C(1)-C(7)	1.4523(14)	C(2)- C(1)-C(7)	121.29(9)	C(15)-C(16)-H(16B)	112.5(7)
C(8)-C(4)	1.4448(14)	C(12)-C(8)-C(11)	117.74(9)	H(16A)-C(16)-H(16B)	110.6(10)
C(18)-H(18)	0.999(14)	C(12)-C(8)-C(4)	119.67(9)		
C(21)-H(21A)	0.968(14)	C(11)-C(8)-C(4)	122.59(9)		
C(21)-H(21C)	0.962(14)	O(17)-C(18)-N(20)	124.88(10)		
C(21)-H(21B)	0.964(16)	O(17)-C(18)-H(18)	122.4(8)		
C(4)-C(5)	1.4122(14)	N(20)-C(18)-H(18)	112.7(8)		
C(15)-C(16)	1.5372(15)	N(20)-C(21)-H(21A)	108.8(8)		
C(15)-H(15A)	0.980(13)	N(20)-C(21)-H(21C)	110.4(8)		
C(15)-H(15B)	0.988(14)	H(21A)-C(21)-H(21C)	109.1(11)		
C(5)-H(5)	0.945(14)	N(20)-C(21)-H(21B)	110.1(9)		
C(22)-H(22A)	0.976(15)	H(21A)-C(21)-H(21B)	107.9(12)		
C(22)-H(22B)	0.979(14)	H(21C)-C(21)-H(21B)	110.4(12)		
C(22)-H(22C)	1.001(14)	C(3)-C(4)-C(5)	117.53(9)		
C(16)-H(16A)	0.961(13)	C(3)-C(4)-C(8)	122.26(9)		
C(16)-H(16B)	0.960(12)	C(5)-C(4)-C(8)	120.20(9)		

Figure S3. Molecular structure showing 99% thermal ellipsoids and the unit cell of **1b**

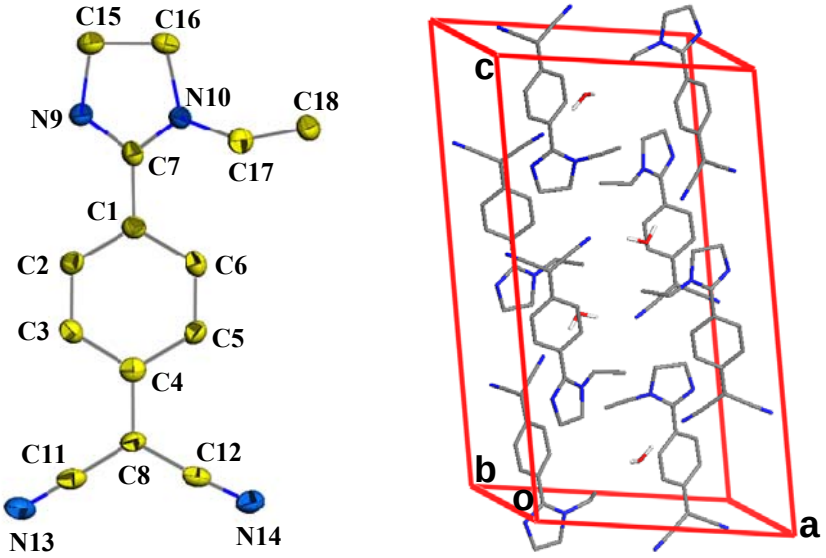

Table S3. Crystallographic details of **1b**

Common name	2-(4-dicyanomethylenecyclohexa-2,5-dieny1idene)-1-ethylimidazolidine. H_2O
Empirical formula	$C_{28}H_{30}N_8O$
Crystal system	Monoclinic
Space group	$P2_1/c$
a / Å	14.7692(12)
b / Å	7.3550(6)
c / Å	24.420(2)
α / deg.	90.00
β / deg.	105.3880(10)
γ /deg.	90.00
V / $Å^3$	2557.6(4)
Z	4
$\rho_{calc.}$ / g cm^{-3}	1.285
μ / cm^{-1}	0.083
Temperature / K	100(2)
λ / Å	0.71073
No. of reflections	4506
No. of parameters	352
Max., Min. transmission	0.990, 0.995
GOF	1.127
R [for $I \geq 2\sigma_I$]	0.0594
wR^2	0.1210
Largest difference peak and hole / e$Å^{-3}$	0.239, 0.048

Table S4. Bond lengths and bond angles for **1b**

Atoms	Bond length (Å)	Atoms	Bond length (Å)	Atoms	Bond length (Å)
N(9)-C(3)	1.317(3)	C(9)-C(12)	1.406(3)	C(19)-C(23)	1.408(3)
N(9)-C(8)	1.458(3)	C(10)-H(10A)	0.9900	C(19)-H(19)	0.9500
N(9)-H(41)	0.91(2)	C(10)-H(10B)	0.9900	C(20)-H(20)	0.9500
N(5)-C(3)	1.324(3)	C(11)-H(11)	0.9500	C(21)-H(21)	0.9500
N(5)-C(14)	1.461(3)	C(13)-C(14)	1.509(3)	C(22)-C(24)	1.402(3)
N(5)-C(10)	1.470(3)	C(13)-H(13A)	0.9800	C(22)-C(23)	1.441(3)
C(1)-C(6)	1.407(3)	C(13)-H(13B)	0.9800	C(24)-N(3)	1.156(3)
C(1)-C(11)	1.411(3)	C(13)-H(13C)	0.9800	C(25)-C(26)	1.525(3)
C(1)-C(9)	1.440(3)	C(14)-H(14A)	0.9900	C(25)-H(25A)	0.9900
C(2)-C(5)	1.398(3)	C(14)-H(14B)	0.9900	C(25)-H(25B)	0.9900
C(2)-C(7)	1.404(3)	N(10)-C(16)	1.326(3)	C(26)-H(26A)	0.9900
C(2)-C(3)	1.462(3)	N(10)-C(25)	1.465(3)	C(26)-H(26B)	0.9900
C(4)-N(2)	1.157(3)	N(10)-H(40)	0.90(3)	C(27)-C(28)	1.512(3)
C(4)-C(9)	1.405(3)	C(15)-C(21)	1.396(3)	C(27)-H(27A)	0.9900
C(5)-C(11)	1.366(3)	C(15)-C(20)	1.398(3)	C(27)-H(27B)	0.9900
C(5)-H(5)	0.9500	C(15)-C(16)	1.460(3)	C(28)-H(28A)	0.9800
C(6)-C(7)	1.377(3)	N(7)-C(16)	1.321(3)	C(28)-H(28B)	0.9800
C(6)-H(6)	0.9500	N(7)-C(27)	1.465(3)	C(28)-H(28C)	0.9800
C(7)-H(7)	0.9500	N(7)-C(26)	1.472(3)		
O(1)-H(43)	0.90(3)	C(17)-C(21)	1.371(3)		
O(1)-H(42)	0.93(4)	C(17)-C(23)	1.404(3)		
N(1)-C(12)	1.155(3)	C(17)-H(17)	0.9500		
C(8)-C(10)	1.529(3)	C(18)-N(4)	1.158(3)		
C(8)-H(8A)	0.9900	C(18)-C(22)	1.404(3)		
C(8)-H(8B)	0.9900	C(19)-C(20)	1.376(3)		

Atoms	Bond angle (°)	Atoms	Bond angle (°)	Atoms	Bond angle (°)
C(3)-N(9)-C(8)	111.87(19)	N(5)-C(10)-H(10B)	111.1	C(19)-C(20)-C(15)	120.8(2)
C(3)-N(9)-H(41)	125.3(14)	C(8)-C(10)-H(10B)	111.1	C(19)-C(20)-H(20)	119.6
C(8)-N(9)-H(41)	122.4(14)	H(10A)-C(10)-H(10B)	109.1	C(15)-C(20)-H(20)	119.6
C(3)-N(5)-C(14)	128.92(19)	C(5)-C(11)-C(1)	121.8(2)	C(17)-C(21)-C(15)	121.2(2)
C(3)-N(5)-C(10)	110.40(18)	C(5)-C(11)-H(11)	119.1	C(17)-C(21)-H(21)	119.4
C(14)-N(5)-C(10)	119.21(18)	C(1)-C(11)-H(11)	119.1	C(15)-C(21)-H(21)	119.4
C(6)-C(1)-C(11)	116.98(19)	N(1)-C(12)-C(9)	177.1(2)	C(24)-C(22)-C(18)	118.73(19)
C(6)-C(1)-C(9)	122.87(19)	C(14)-C(13)-H(13A)	109.5	C(24)-C(22)-C(23)	121.27(19)
C(11)-C(1)-C(9)	120.15(19)	C(14)-C(13)-H(13B)	109.5	C(18)-C(22)-C(23)	119.99(19)
C(5)-C(2)-C(7)	118.25(19)	H(13A)-C(13)-H(13B)	109.5	C(17)-C(23)-C(19)	116.99(19)
C(5)-C(2)-C(3)	120.64(19)	C(14)-C(13)-H(13C)	109.5	C(17)-C(23)-C(22)	122.25(19)
C(7)-C(2)-C(3)	120.91(19)	H(13A)-C(13)-H(13C)	109.5	C(19)-C(23)-C(22)	120.77(19)
N(9)-C(3)-N(5)	111.72(19)	H(13B)-C(13)-H(13C)	109.5	N(3)-C(24)-C(22)	178.2(2)
N(9)-C(3)-C(2)	122.3(2)	N(5)-C(14)-C(13)	113.4(2)	N(10)-C(25)-C(26)	102.30(17)
N(5)-C(3)-C(2)	126.0(2)	N(5)-C(14)-H(14A)	108.9	N(10)-C(25)-H(25A)	111.3
N(2)-C(4)-C(9)	179.0(3)	C(13)-C(14)-H(14A)	108.9	C(26)-C(25)-H(25A)	111.3
C(11)-C(5)-C(2)	120.8(2)	N(5)-C(14)-H(14B)	108.9	N(10)-C(25)-H(25B)	111.3
C(11)-C(5)-H(5)	119.6	C(13)-C(14)-H(14B)	108.9	C(26)-C(25)-H(25B)	111.3
C(2)-C(5)-H(5)	119.6	H(14A)-C(14)-H(14B)	107.7	H(25A)-C(25)-H(25B)	109.2
C(7)-C(6)-C(1)	121.3(2)	C(16)-N(10)-C(25)	111.02(18)	N(7)-C(26)-C(25)	102.39(17)
C(7)-C(6)-H(6)	119.4	C(16)-N(10)-H(40)	123.6(16)	N(7)-C(26)-H(26A)	111.3
C(1)-C(6)-H(6)	119.4	C(25)-N(10)-H(40)	122.8(16)	C(25)-C(26)-H(26A)	111.3
C(6)-C(7)-C(2)	120.8(2)	C(21)-C(15)-C(20)	118.05(19)	N(7)-C(26)-H(26B)	111.3
C(6)-C(7)-H(7)	119.6	C(21)-C(15)-C(16)	119.74(19)	C(25)-C(26)-H(26B)	111.3
C(2)-C(7)-H(7)	119.6	C(20)-C(15)-C(16)	122.13(19)	H(26A)-C(26)-H(26B)	109.2
H(43)-O(1)-H(42)	103(3)	C(16)-N(7)-C(27)	129.40(18)	N(7)-C(27)-C(28)	112.86(18)
N(9)-C(8)-C(10)	102.48(17)	C(16)-N(7)-C(26)	110.55(17)	N(7)-C(27)-H(27A)	109.0
N(9)-C(8)-H(8A)	111.3	C(27)-N(7)-C(26)	120.02(17)	C(28)-C(27)-H(27A)	109.0
C(10)-C(8)-H(8A)	111.3	N(7)-C(16)-N(10)	111.24(19)	N(7)-C(27)-H(27B)	109.0
N(9)-C(8)-H(8B)	111.3	N(7)-C(16)-C(15)	127.08(19)	C(28)-C(27)-H(27B)	109.0
C(10)-C(8)-H(8B)	111.3	N(10)-C(16)-C(15)	121.68(19)	H(27A)-C(27)-H(27B)	107.8
H(8A)-C(8)-H(8B)	109.2	C(21)-C(17)-C(23)	121.5(2)	C(27)-C(28)-H(28A)	109.5
C(4)-C(9)-C(12)	116.84(19)	C(21)-C(17)-H(17)	119.3	C(27)-C(28)-H(28B)	109.5
C(4)-C(9)-C(1)	122.81(19)	C(23)-C(17)-H(17)	119.3	H(28A)-C(28)-H(28B)	109.5
C(12)-C(9)-C(1)	120.33(19)	N(4)-C(18)-C(22)	176.2(2)	C(27)-C(28)-H(28C)	109.5
N(5)-C(10)-C(8)	103.35(17)	C(20)-C(19)-C(23)	121.5(2)	H(28A)-C(28)-H(28C)	109.5
N(5)-C(10)-H(10A)	111.1	C(20)-C(19)-H(19)	119.3	H(28B)-C(28)-H(28C)	109.5
C(8)-C(10)-H(10A)	111.1	C(23)-C(19)-H(19)	119.3		

Figure S4. Molecular structure showing 99% thermal ellipsoids and the unit cell of **1c**

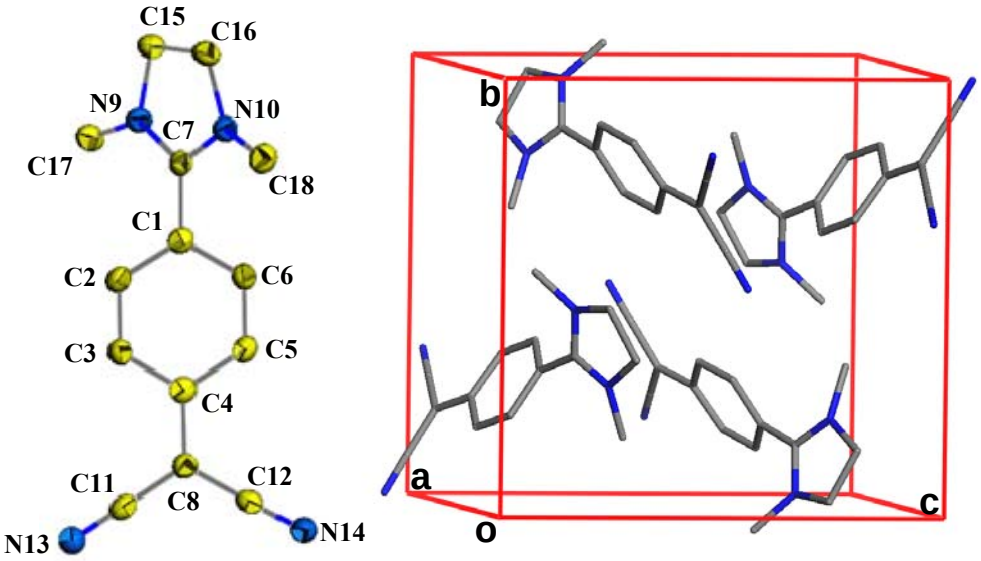

Table S5. Crystallographic details of **1c**

Common name	2-(4-dicyanomethylenecyclohexa-2,5-dieny1idene)-1,3-dimethylimidazolidine
Empirical formula	$C_{14}H_{14}N_4$
Crystal system	Monoclinic
Space group	$P2_1/c$
a / Å	9.1349(6)
b / Å	11.5867(7)
c / Å	11.7632(7)
α / deg.	90.00
β / deg.	98.4420(10)
γ /deg.	90.00
V / Å^3	1231.57(13)
Z	4
$\rho_{calc.}$ / g cm^{-3}	1.285
μ / cm^{-1}	0.081
Temperature / K	100(2)
λ / Å	0.71073
No. of reflections	2165
No. of parameters	165
Max., Min. transmission	0.978, 0.992
GOF	1.05
R [for $I \geq 2\sigma_I$]	0.0353
wR^2	0.0905
Largest difference peak and hole / eÅ^{-3}	0.157, 0.041

Table S6. Bond lengths and bond angles for **1c**

Atoms	Bond length (Å)	Atoms	Bond angle (°)	Atoms	Bond angle (°)
N(2)-C(12)	1.3157(15)	C(12)-N(2)-C(14)	127.41(10)	N(4)-C(8)-C(1)	178.22(13)
N(2)-C(14)	1.4560(16)	C(12)-N(2)-C(9)	111.21(10)	N(2)-C(9)-C(11)	102.72(9)
N(2)-C(9)	1.4671(15)	C(14)-N(2)-C(9)	121.09(10)	C(5)-C(10)-C(2)	121.65(11)
N(1)-C(12)	1.3304(16)	C(12)-N(1)-C(13)	126.41(10)	N(1)-C(11)-C(9)	103.04(9)
N(1)-C(13)	1.4516(16)	C(12)-N(1)-C(11)	110.15(10)	N(2)-C(12)-N(1)	111.94(11)
N(1)-C(11)	1.4700(15)	C(13)-N(1)-C(11)	118.01(10)	N(2)-C(12)-C(6)	124.52(11)
C(1)-C(8)	1.4062(17)	C(8)-C(1)-C(3)	117.08(11)	N(1)-C(12)-C(6)	123.53(11)
C(1)-C(3)	1.4104(17)	C(8)-C(1)-C(2)	120.78(11)	N(4)-C(8)-C(1)	178.22(13)
C(1)-C(2)	1.4391(17)	C(3)-C(1)-C(2)	122.12(11)		
C(2)-C(10)	1.4107(17)	C(10)-C(2)-C(4)	116.80(11)		
C(2)-C(4)	1.4099(17)	C(10)-C(2)-C(1)	122.15(11)		
C(3)-N(3)	1.1579(16)	C(4)-C(2)-C(1)	121.04(11)		
C(4)-C(7)	1.3761(17)	N(3)-C(3)-C(1)	179.00(13)		
N(4)-C(8)	1.1577(16)	C(7)-C(4)-C(2)	121.57(11)		
C(5)-C(10)	1.3815(17)	C(10)-C(5)-C(6)	120.43(11)		
C(5)-C(6)	1.3997(17)	C(7)-C(6)-C(5)	118.62(11)		
C(6)-C(7)	1.3950(17)	C(7)-C(6)-C(12)	120.44(11)		
C(6)-C(12)	1.4633(16)	C(5)-C(6)-C(12)	120.93(11)		
C(9)-C(11)	1.5290(17)	C(4)-C(7)-C(6)	120.90(11)		

Absorption and Emission Spectroscopy

Electronic absorption spectra of solutions (in transmission mode) and solid (in diffuse reflectance mode) were recorded on a Varian model Cary 100 UV-Vis spectrometer; the reflectance spectra were converted to absorption spectra using the Kubelka-Munk function. Steady-state fluorescence emission and excitation spectra were recorded on a Horiba Jobin Yvon model FL3-22 Fluorolog spectrofluorimeter, in right angle geometry. The microcrystalline solid in the form of KBr pellet was mounted on a solid sample holder. Optical density of the samples was maintained below 0.2 in order to avoid inner-filter effects. Fluorescence quantum yield of solution was determined using quinine sulfate in 1N H_2SO_4 ($\Phi = 0.546$) as the standard; absolute values of the quantum yield of solid samples were determined using an integrating sphere and the PLQY Calculator v.3 software (Jobin Yvon).

Figure S5. Photographs of solid samples (KBr pellet) of **1a-c** under ambient and UV (365 nm) light; solutions, even with OD ~ 0.1 show no visible fluorescence.

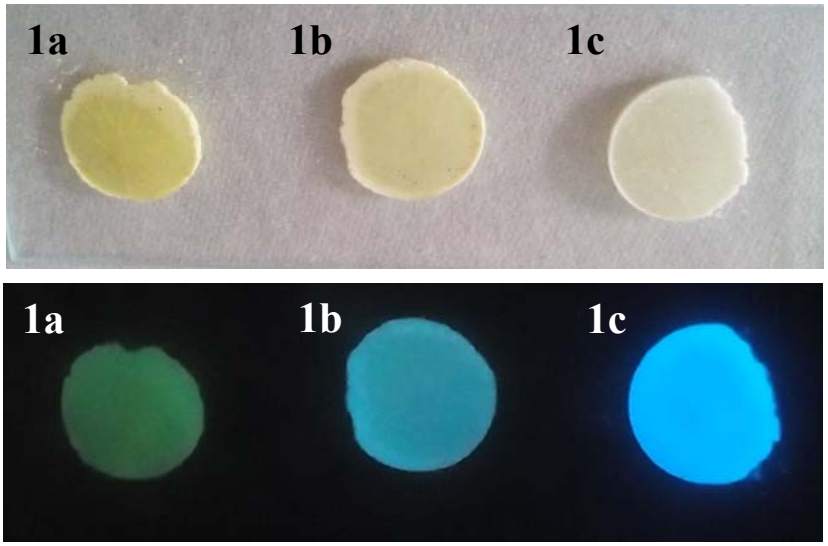

Figure S6. Fluorescence excitation spectra of solution and solid **1a-c**

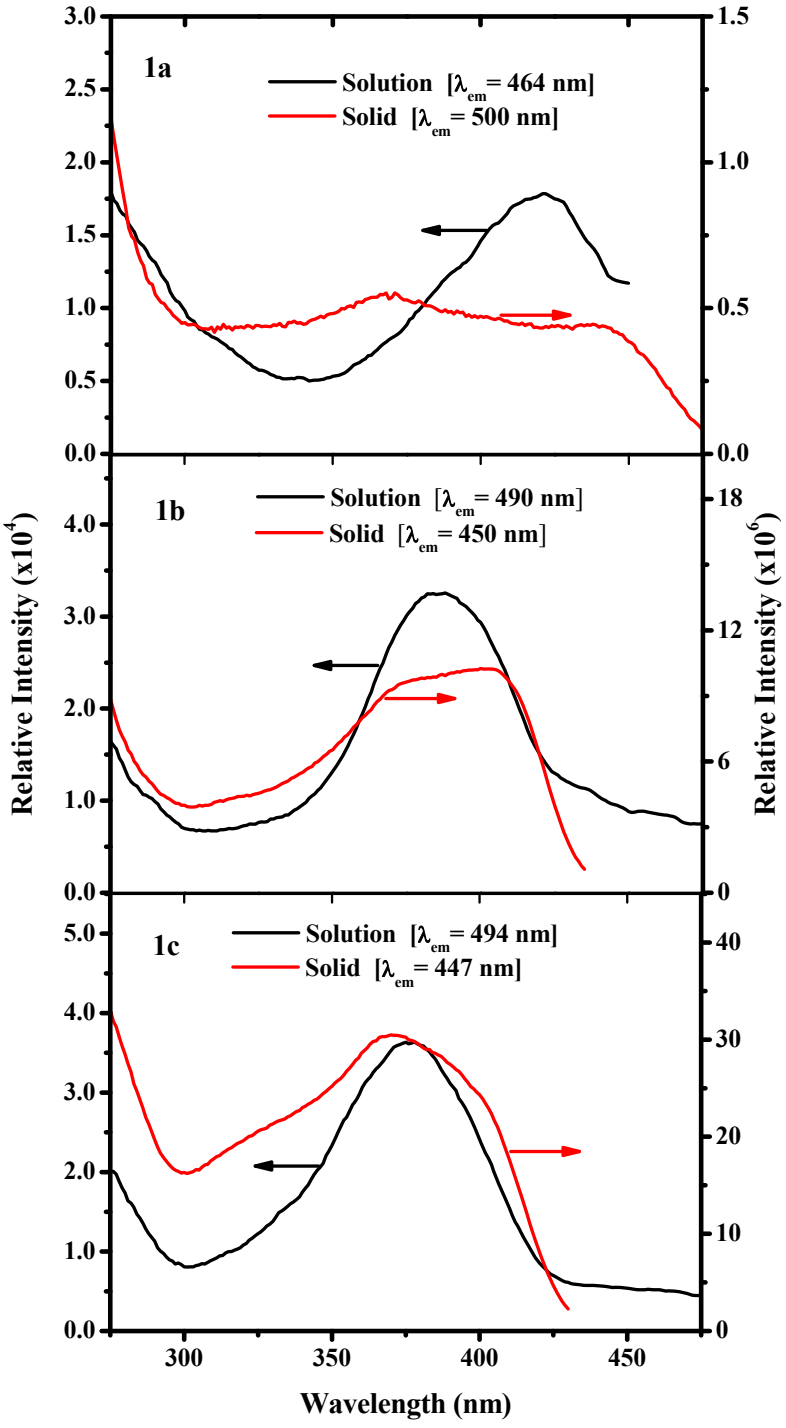

Solvatochromism data

Absorption spectra of **1a-c** were recorded in methanol (Reichardt parameter, E_T^N = 0.762), acetonitrile (E_T^N = 0.460), acetone (E_T^N = 0.355) and ethyl acetate (E_T^N = 0.228) solvents to study the solvatochromic effect. The spectra show clear blue shift with increasing solvent polarity.

Figure S7. Absorption spectra of **1a-c** in solvents of varying polarity.

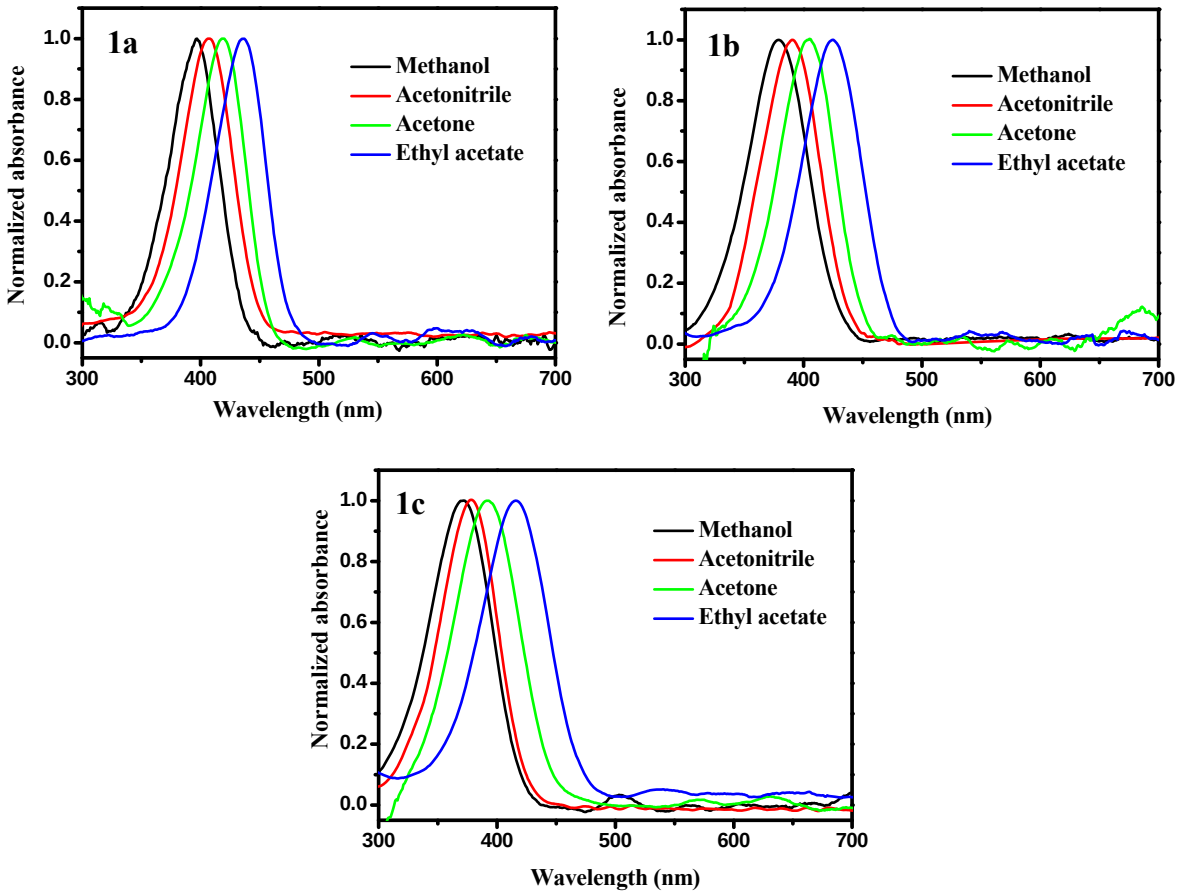

Computational Details

Methods

Gaussian 09 (Revision C.01)* was used for all the geometry optimization studies. Computations were carried out at the B3LYP/6-31G* level; TD-DFT method was used for the excited states and SCRF to model the environment effect. Full as well as partial optimization computations were carried out as described in the main text. The full optimization used the molecular structure from the crystal structure analysis for the initial geometry.

Partial optimization calculations for the ground state started with the molecular structure from the crystal structure analysis as the initial geometry with the torsion angle, φ frozen; in **1b**, the optimized geometry corresponded to the $\theta = 30^o$ point, whereas in **1a** and **1c** these were at $\theta = 7^o$ and 45^o respectively. θ was fixed at 10^o intervals (starting with 10^o, 30^o and 40^o respectively in **1a**, **1b** and **1c**), each optimization carried out using the previous point geometry as the initial one. These calculations, together with single point TD-DFT calculation at the partially optimized geometry, generated the $S_0(G)$ and $S_1(G)$ profiles. The partially optimized geometry corresponding to the minimum of the $S_0(G)$ profile was used to optimize the excited state geometry (keyword ROOT=1), again freezing the φ angle. Following the protocol as in the case of the ground state geometry, the $S_0(E)$ and $S_1(E)$ profiles were computed.

Default thresholds (0.0003) were used for all geometry optimizations. However, the partial optimization of the excited state structures of **1a** with $\theta = 70^o$, 80^o and 90^o (on the $S_1(E)$ profile in Fig. 5a) failed to converge, possibly because these are far from minimum energy geometries. The optimizations were attempted with lower thresholds and were successful with threshold values of 0.003, for the 70^o and 80^o points; these are shown for **1a** in Fig. 5a. Even with this lowered optimization threshold, the $\theta = 90^o$ structure could not be optimized, and hence was abandoned and not shown in the figure.

* M. J. Frisch, G. W. Trucks, H. B. Schlegel, G. E. Scuseria, M. A. Robb, J. R. Cheeseman, G. Scalmani, V. Barone, B. Mennucci, G. A. Petersson, H. Nakatsuji, M. Caricato, X. Li, H. P. Hratchian, A. F. Izmaylov, J. Bloino, G. Zheng, J. L. Sonnenberg, M. Hada, M. Ehara, K. Toyota, R. Fukuda, J. Hasegawa, M. Ishida, T. Nakajima, Y. Honda, O. Kitao, H. Nakai, T. Vreven, J. A. Montgomery, Jr., J. E. Peralta, F. Ogliaro, M. Bearpark, J. J. Heyd, E. Brothers, K. N. Kudin, V. N. Staroverov, T. Keith, R. Kobayashi, J. Normand, K. Raghavachari, A. Rendell, J. C. Burant, S. S. Iyengar, J. Tomasi, M. Cossi, N. Rega, J. M. Millam, M. Klene, J. E. Knox, J. B. Cross, V. Bakken, C. Adamo, J. Jaramillo, R. Gomperts, R. E. Stratmann, O. Yazyev, A. J. Austin, R. Cammi, C. Pomelli, J. W. Ochterski, R. L. Martin, K. Morokuma, V. G. Zakrzewski, G. A. Voth, P. Salvador, J. J. Dannenberg, S. Dapprich, A. D. Daniels, O. Farkas, J. B. Foresman, J. V. Ortiz, J. Cioslowski, and D. J. Fox, Gaussian 09, Revision C.01, Gaussian, Inc., Wallingford CT, 2010.

Fully optimized ground and excited states

Figure S8. Fully optimized [B3LYP/6-31G*; SCRF (acetonitrile)] **(a)** ground state and **(b)** excited state geometries of molecules **1a-c**

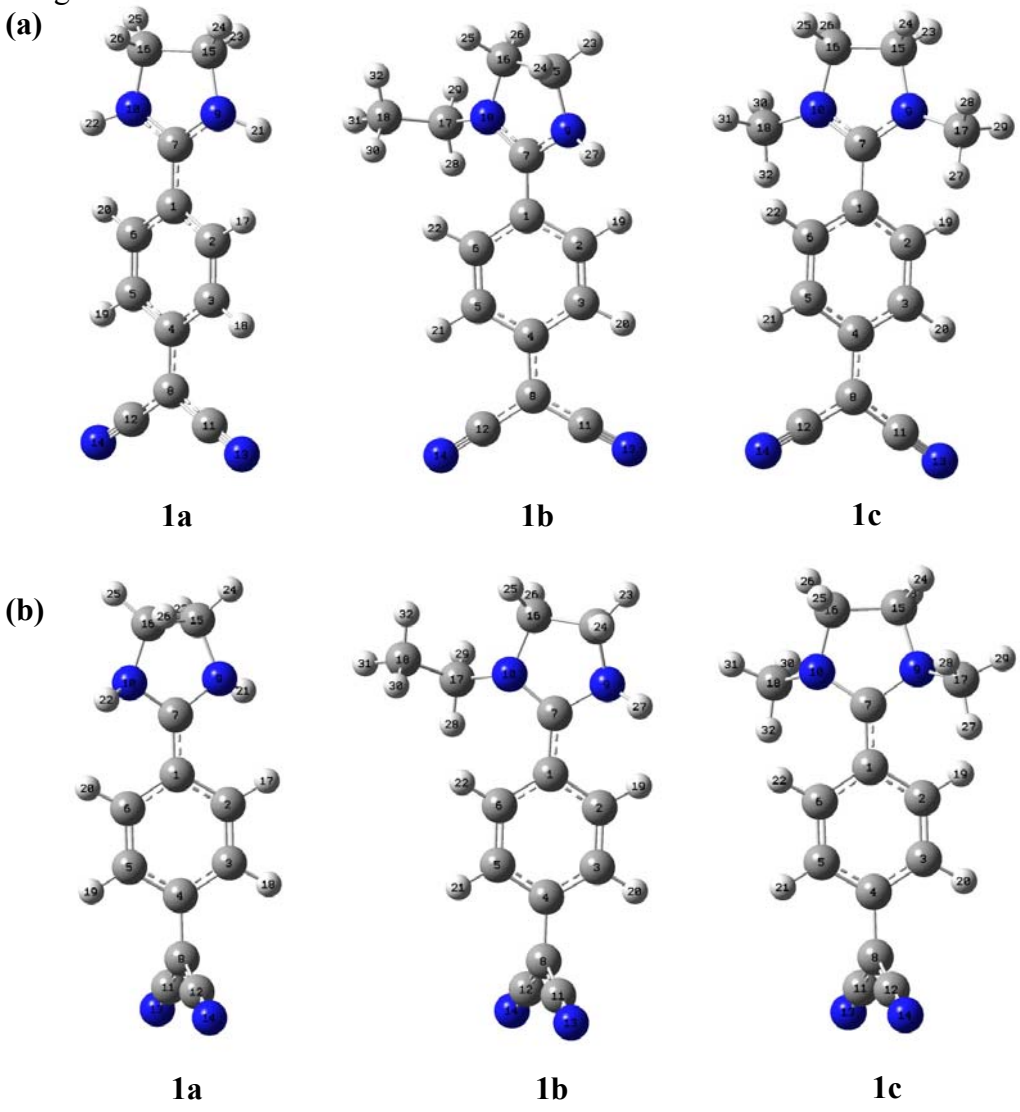

Table S7. Computed [B3LYP/6-31G*; SCRF (acetonitrile)] absorption energy (wavelength maximum, λ_{max}^{abs}) and oscillator strength (f) for the first three excited states of the fully optimized ground state structures of **1a-c** (shown in Fig. S8a).

Molecule	$S_0 \rightarrow S_1$		$S_0 \rightarrow S_2$		$S_0 \rightarrow S_3$	
	λ_{max}^{abs} (nm)	f	λ_{max}^{abs} (nm)	f	λ_{max}^{abs} (nm)	f
1a	421	1.092	312	0.004	290	0.000
1b	416	0.986	317	0.006	293	0.000
1c	385	0.702	317	0.003	295	0.000

Table S8. Computed [B3LYP/6-31G*; SCRF (acetonitrile)] emission energy (wavelength maximum, λ_{max}^{em}) and oscillator strength (f) for the first three excited states of the fully optimized excited state structures of **1a-c** (shown in Fig. S8b).

Molecule	$S_1 \rightarrow S_0$		$S_2 \rightarrow S_0$		$S_3 \rightarrow S_0$	
	λ_{max}^{em} (nm)	f	λ_{max}^{em} (nm)	f	λ_{max}^{em} (nm)	f
1a	1107	0.000	386	0.002	304	0.039
1b	1065	0.000	389	0.002	314	0.000
1c	1093	0.000	386	0.002	324	0.000

Table S9. Computed [B3LYP/6-31G*; SCRF (acetonitrile)] emission energy (wavelength maximum, λ_{max}^{em}) and oscillator strength (f) for the first three excited states of the partially optimized (with θ and φ fixed at the values of fully optimized ground state geometry) excited state structures of **1a-c**.

Molecule	$S_1 \rightarrow S_0$		$S_2 \rightarrow S_0$		$S_3 \rightarrow S_0$	
	λ_{max}^{em} (nm)	f	λ_{max}^{em} (nm)	f	λ_{max}^{em} (nm)	f
1a	463	0.999	320	0.002	293	0.000
1b	475	0.858	326	0.003	295	0.000
1c	501	0.634	329	0.004	296	0.000

Computed transition dipole moments

Figure S9. Calculated [B3LYP/6-31G*, TD-DFT (ROOT=1)] transition dipole moments of the molecules **1a-c** with the geometry taken from the crystal structure (**1a** in vacuum, **1b** in propanonitrile and **1c** in acetonitrile environments).

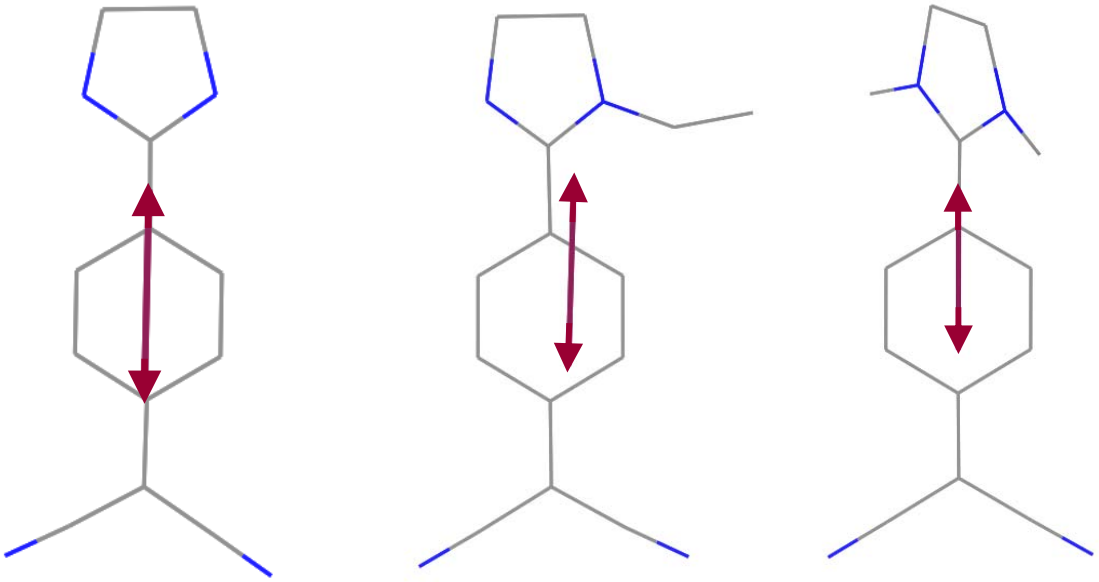

1a **1b** **1c**

Frequencies calculated for the fully optimized structures

Table S10. Computed frequencies of the fully optimized structure of **1a** in vacuum and acetonitrile environments (all positive, indicating that these are genuine energy minimum structures)

No.	Frequency (cm^{-1})		No.	Frequency (cm^{-1})		No.	Frequency (cm^{-1})	
	Acetonitrile	Vacuum		Acetonitrile	Vacuum		Acetonitrile	Vacuum
1	47.9	45.4	26	733.8	724.0	51	1405.0	1427.0
2	57.2	61.7	27	750.1	745.7	52	1411.3	1437.6
3	85.9	86.7	28	829.6	809.8	53	1498.4	1495.0
4	91.7	109.9	29	851.1	850.1	54	1528.7	1533.8
5	127.3	127.5	30	897.7	908.8	55	1538.9	1542.7
6	131.6	130.2	31	921.7	915.2	56	1550.2	1555.9
7	155.6	157.5	32	959.3	958.4	57	1558.8	1556.2
8	169.0	201.4	33	969.8	970.4	58	1597.2	1565.0
9	211.2	208.2	34	977.9	981.6	59	1622.3	1652.0
10	284.7	288.9	35	1012.8	1002.2	60	1658.9	1676.3
11	302.0	289.1	36	1026.0	1005.4	61	2253.1	2297.3
12	340.6	336.8	37	1031.5	1049.3	62	2288.7	2318.9
13	420.6	425.6	38	1059.1	1051.6	63	3079.2	3037.6
14	440.6	444.7	39	1135.2	1131.9	64	3082.7	3045.4
15	499.0	475.6	40	1156.6	1142.2	65	3147.5	3125.6
16	507.6	487.1	41	1162.6	1157.1	66	3156.5	3132.1
17	512.4	519.8	42	1227.0	1223.7	67	3196.9	3179.1
18	524.2	521.2	43	1228.1	1236.2	68	3197.5	3179.5
19	544.6	538.8	44	1249.7	1236.6	69	3213.6	3217.7
20	556.5	586.8	45	1254.3	1247.9	70	3215.5	3218.7
21	617.3	617.4	46	1327.6	1312.6	71	3637.7	3626.8
22	635.7	623.6	47	1329.7	1347.6	72	3640. 6	3627.1
23	645.2	638.6	48	1355.5	1349.4			
24	689.7	667.9	49	1361.0	1363.5			
25	729.1	723.2	50	1373.7	1406.5			

Table S11. Computed frequencies of the fully optimized structure of **1b** in propanonitrile and acetonitrile environments (all positive, indicating that these are genuine energy minimum structures)

No.	Frequency (cm^{-1})		No.	Frequency (cm^{-1})		No.	Frequency (cm^{-1})	
	Acetonitrile	Propanonitrile		Acetonitrile	Propanonitrile		Acetonitrile	Propanonitrile
1	33.4	33.8	31	746.6	746.5	61	1401.3	1401.3
2	48.6	48.6	32	792.5	792.5	62	1409.3	1409.4
3	66.7	67.0	33	805.1	805.1	63	1439.7	1439.9
4	78.0	78.3	34	841.7	841.6	64	1492.6	1493.1
5	100.5	100.6	35	856.0	856.1	65	1508.7	1508.9
6	103.0	103.2	36	886.6	886.3	66	1513.0	1513.1
7	126.8	126.9	37	951.4	951.4	67	1526.8	1526.8
8	130.2	130.2	38	970.6	970.5	68	1529.7	1529.7
9	150.4	150.5	39	978.5	978.4	69	1533.5	1533.5
10	164.5	164.7	40	984.8	984.8	70	1549.6	1549.6
11	216.7	216.8	41	999.6	999.5	71	1560.1	1559.8
12	226.8	226.8	42	1013.7	1013.6	72	1594.1	1593.9
13	271.0	271.1	43	1028.4	1028.3	73	1609.2	1609.0
14	282.8	282.8	44	1055.5	1055.6	74	1652.7	1652.8
15	346.7	346.6	45	1107.2	1107.3	75	2248.7	2249.1
16	367.8	367.8	46	1124.6	1124.6	76	2285.9	2286.1
17	378.8	378.8	47	1144.4	1144.5	77	3062.2	3062.2
18	428.7	428.8	48	1159.6	1159.7	78	3065.1	3065.0
19	479.5	479.5	49	1212.5	1212.5	79	3071.9	3071.7
20	510.1	510.0	50	1222.3	1222.1	80	3085.0	3084.7
21	513.1	513.2	51	1231.4	1231.4	81	3129.1	3129.1
22	520.5	520.6	52	1240.1	1240.2	82	3137.0	3136.7
23	539.5	539.7	53	1252.2	1252.1	83	3138.1	3138.2
24	560.6	561.4	54	1279.3	1279.2	84	3148.6	3148.5
25	617.8	617.9	55	1323.2	1323.2	85	3159.3	3159.3
26	634.8	634.8	56	1333.1	1333.1	86	3197.7	3197.7
27	636.7	636.5	57	1558.8	1352.6	87	3204.6	3204.7
28	646.0	646.0	58	1597.2	1359.4	88	3213.1	3213.2
29	695.8	695.7	59	1622.3	1368.3	89	3222.4	3222.5
30	736.2	736.1	60	1658.9	1376.8	90	3629.8	3629.8

Table S12. Computed frequencies of the fully optimized structure of **1c** in acetonitrile environment (all positive, indicating that this is a genuine energy minimum structure)

No.	Frequency (cm^{-1})	No.	Frequency (cm^{-1})	No.	Frequency (cm^{-1})	No.	Frequency (cm^{-1})
	Acetonitrile		Acetonitrile		Acetonitrile		Acetonitrile
1	35.8	24	542.5	47	1164.1	70	1551.8
2	43.8	25	608.9	48	1173.1	71	1568.8
3	66.7	26	618.0	49	1214.6	72	1604.3
4	69.7	27	637.2	50	1240.9	73	1626.7
5	102.2	28	641.9	51	1253.2	74	1649.1
6	105.2	29	663.8	52	1253.6	75	2244.2
7	124.2	30	698.2	53	1257.3	76	2283.3
8	127.9	31	742.2	54	1278.5	77	3064.6
9	132.8	32	745.5	55	1319.2	78	3065.5
10	140.9	33	844.3	56	1341.8	79	3077.8
11	192.1	34	853.9	57	1351.4	80	3081.5
12	192.4	35	866.7	58	1357.0	81	3120.0
13	229.4	36	950.6	59	1362.9	82	3124.0
14	251.6	37	970.5	60	1408.8	83	3125.0
15	285.1	38	977.4	61	1463.5	84	3135.7
16	347.1	39	985.6	62	1473.8	85	3192.2
17	352.8	40	1010.8	63	1485.4	86	3192.4
18	371.1	41	1015.6	64	1503.6	87	3198.3
19	428.3	42	1029.4	65	1506.0	88	3199.2
20	475.2	43	1102.7	66	1511.2	89	3212.5
21	508.1	44	1104. 3	67	1520.8	90	3214.4
22	511.0	45	1118.5	68	1530.8		
23	525.5	46	1155.0	69	1539.0		

Computed oscillator strengths

Figure S10. Oscillator strength computed for the $S_0 \leftarrow S_1$, $S_0 \leftarrow S_2$, $S_0 \leftarrow S_3$ transitions of the excited state geometries (partially optimized, fixing the angle, φ at the value in the crystal structure and with different values of θ) of **1a-c**.

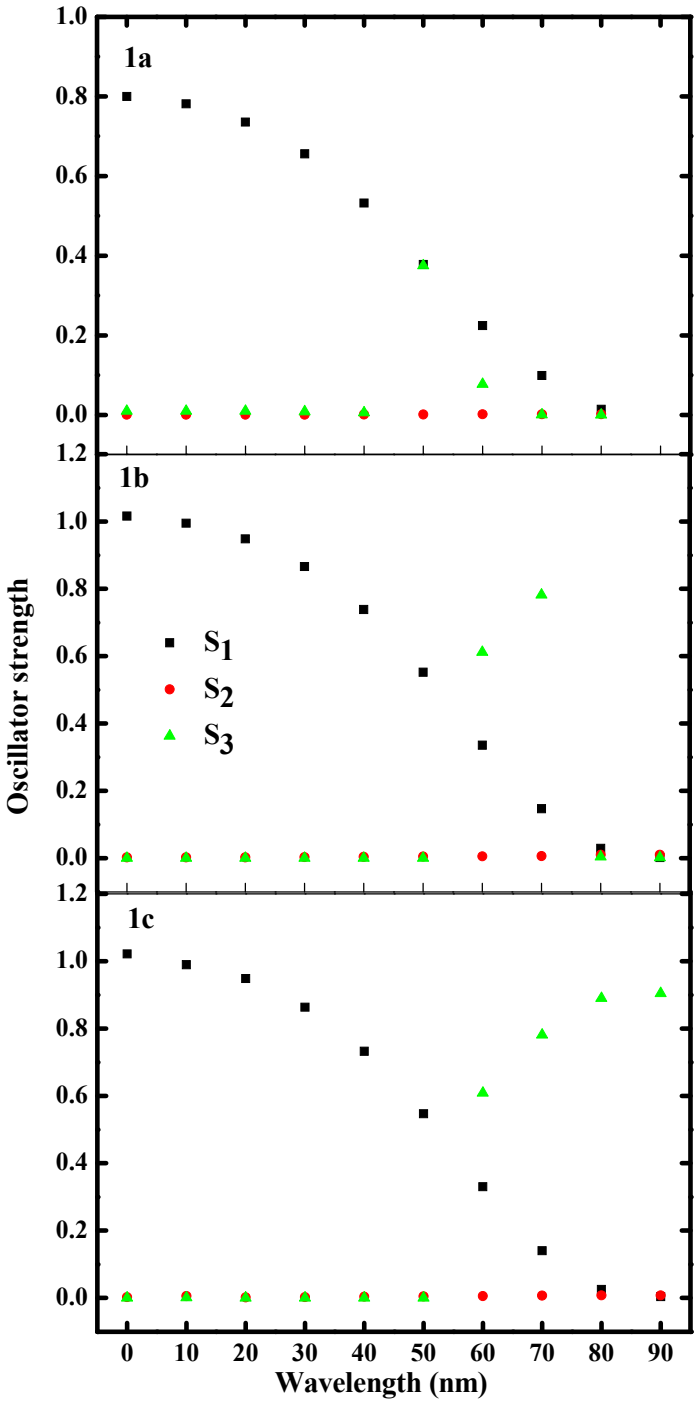

Lattice energy calculations

Materials Studio (v 6.0.0, Accelrys Software Inc.) with GULP module* and Dreiding force field was used for all the computations. A cluster of molecules (54 in **1a**, 61 in **1b**, 55 in **1c**) excised from the crystal lattice was used with torsional angle rotations imposed on one molecule deeply embedded in the middle of the cluster.

*J. D. Gale, A. L. Rohl, The General Utility Lattice Program (GULP), *Molecular Simulation*, **2003**, *29*, 291-341.

Figure S11. Variation of the lattice energy as a function of the twist angle **(a)** φ and **(b)** θ (see Fig. 2 in main text) for the crystals **1a-c**.

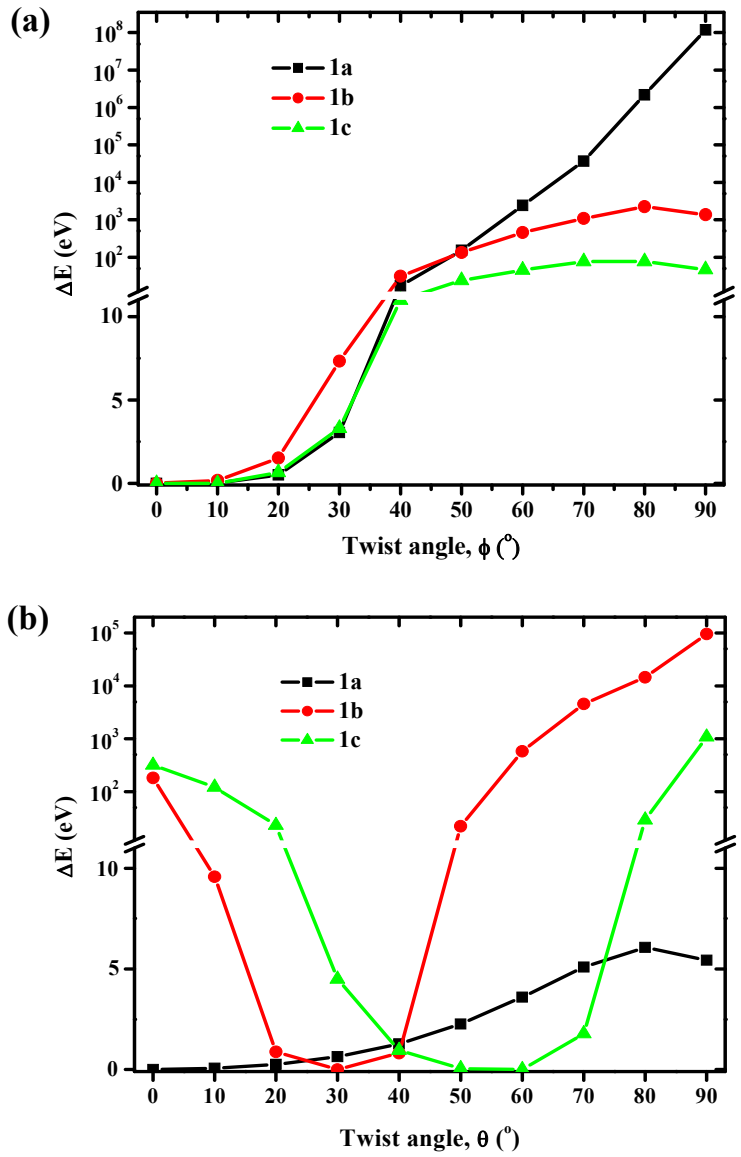

Trends in Energy Transfer Rates

Förster resonance energy transfer

As shown on page S17, the computed transition dipole moment in each of the molecules **1a-c** coincides closely with the molecular dipole axis along the diaminomethylene carbon – dicyanomethylene carbon axis (C7-C8 axis in Figs. S2-S4). The computed transition dipole was used in the following calculations.

In view of the similar overlap between the absorption and emission spectra across the series, dependence of the rate of energy transfer on the relative orientation of the transition dipoles is given by,

$$k_{ET}(Förster) \propto \frac{\kappa^2}{R^6} = \frac{(cos\alpha_{12} - 3 * cos\alpha_1 * cos\alpha_2)^2}{R^6}$$

where α_{12} is the angle between the transition dipoles of molecules 1 and 2, α_1 and α_2 are the angles between the transition dipoles and the vector connecting the two, and R is the distance between the transition dipoles (Fig. S12).

Figure S12. Schematic diagram showing the transition dipoles and the relevant geometric parameters.

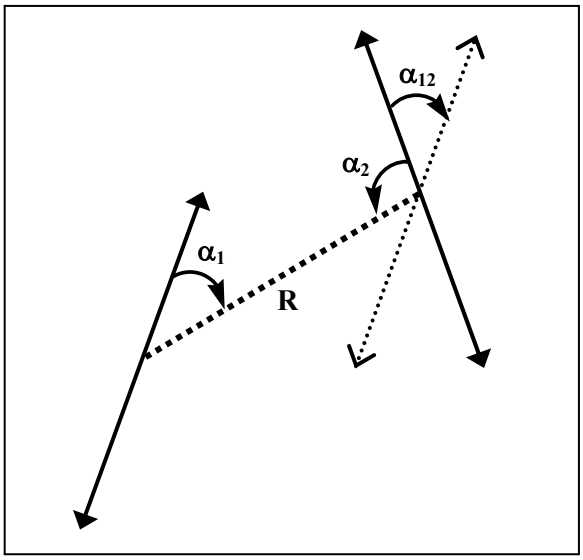

For each crystal, the neighboring molecules with transition dipoles within a distance (R) of 10 Å, around that of a selected molecule in the crystal lattice were considered, to estimate the values of $\frac{\kappa^2}{R^6}$ listed in Table S13. The sum for each crystal and the relative values across the series are shown.

Table S13. The relevant geometric parameters (for molecules within a distance (R) of 10 Å from a reference molecule) and the relative rates of Förster energy transfer in crystals of **1a-c**.

Crystal	R (Å)	α_{12} (°)	α_1 (°)	α_2 (°)	κ	$\frac{\kappa^2}{R^6}$ (10^{-6})	Relative rate
1a	3.860	0.0	87.3	87.3	0.9934	298.356	**1.00**
	5.629	0.0	71. 7	71.7	0.7038	15.572	
	5.630	0.0	71. 7	71.7	0.7038	15.555	
	6.491	0.0	72.5	72.5	0.7293	7.111	
	7.145	0.0	77.2	77.2	0.8518	5.454	
	7.465	0.0	82.1	82.1	0.9426	5.134	
	8.019	0.0	84.7	84.7	0.9747	3.573	
					Total	**350.755**	
1b	6.061	3.1	36.9	34.2	-0.9869	19.648	**0.202**
	6.507	2.4	34.7	37.4	-0.9614	12.177	
	7.161	3.1	60.0	61.8	0.2896	0.623	
	7.198	0.0	75.7	75.7	0.8178	4.809	
	7.355	0.0	86.9	86.1	0.9860	6.142	
	7.355	0.0	86. 9	86.1	0.9860	6.142	
	7.626	0.0	80.4	80.4	0.9165	4.271	
	7.727	5.3	28.0	22.7	-1.4487	9.860	
	8.465	5.3	30.1	34.6	-1.1422	3.546	
	7.812	3.1	75.1	76.2	0.8137	2.913	
	9.665	3.0	71.4	70.5	0.6796	0.567	
					Total	**70.697**	
1c	5.911	0.00	86.4	86.4	0.9882	22.895	**0.130**
	5.969	35.03	54.3	61.3	-0.0222	0.011	
	5.969	35.03	61.3	54.3	-0.0222	0.011	
	6.272	35.04	86.5	60.3	0.7292	8.734	
	6.272	35.03	60.3	86.5	0.7293	8.737	
	9.135	0.00	31.0	31.0	-1.2025	2.489	
	9.135	0.00	31.0	31.0	-1.2025	2.489	
	7.647	0.00	59.7	59.7	0.2363	0.279	
	9.563	0.00	51.3	51.3	-0.1730	0.039	
					Total	**45.683**	

Dexter energy transfer

In order to assess the impact of distances and relative orientations of molecules in the crystals on the Dexter energy transfer rate, a common protocol to define the relevant fluorophores is required. As a reasonable approximation for a uniform model across the series of molecules, the moiety consisting of the benzenoid ring and the diaminomethylene (C7) and dicyanomethylene (C8) carbon atoms (Figs. S2- S4) was chosen to define the molecular plane and the centroid of this moiety to measure the distances.

In view of the similar overlap between the absorption and emission spectra across the series, dependence of the rate of energy transfer on the relative molecular orientations is given by,

$$k_{ET}(Dexter) \propto Se^{-r'} = cos\delta.cos\alpha.\boldsymbol{e^{-r'}} = cos\delta.cos\alpha\boldsymbol{e^{-rcos\alpha}}$$

where r' is the perpendicular distance between the mean planes of the molecules, r is the distance between the centroids, α is the angle between the normal to the mean plane of the reference molecule and the vector connecting the centroids of the two molecules, δ is the angle between the mean planes of molecules 1 and 2 (Fig. S13). Overlap of the relevant wave functions on the two molecules that leads to the Dexter energy transfer decreases exponentially with the distance between the molecular planes (r'). The overlap would be a maximum when the planes are parallel and exactly on top of each other, in a sandwich configuration; slip of the molecule (α increasing from 0^o) and tilt of the planes away from parallel (δ increasing from 0^o) decrease the overlap and can be modeled by the functions cosα and cosδ respectively.

Figure S13. Schematic diagram showing the molecular mean planes and the relevant geometric parameters.

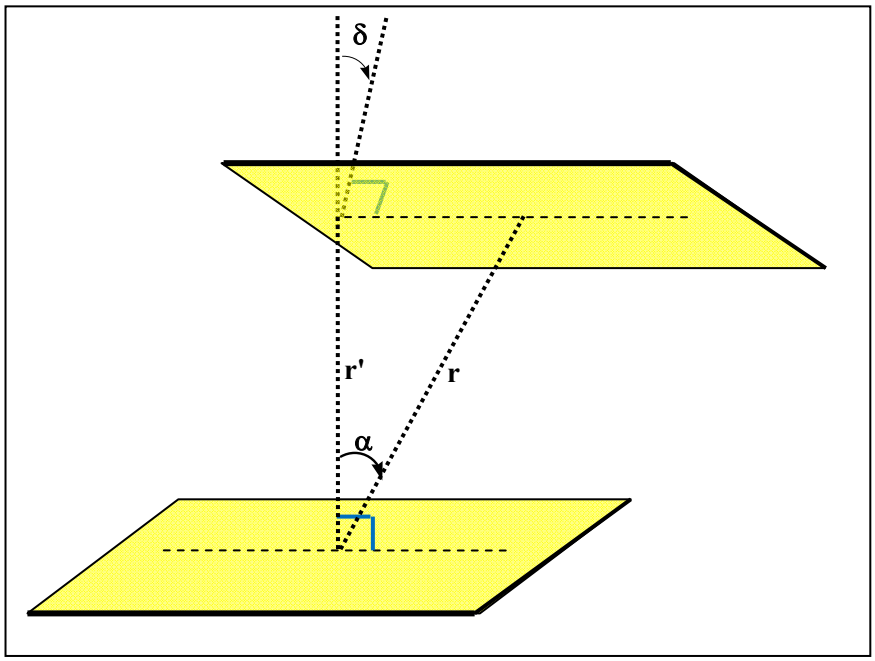

For each crystal, the neighboring molecules with r.sinα < 10 Å [r.sinα = displacement of the centroid of one molecule with respect to the centroid of the other; 10 Å = the approximate length of the diaminodicyanoquinodimethane chromophore; if r.sinα > 10 Å, there is likely to be negligible overlap between the two molecules] and r' in the range 2.5 to 4.5 Å [meaningful π-stacking distance range] around a selected molecule in the crystal lattice were considered, to estimate the values of $Se^{-r'}$ listed in Table S14. The sum for each crystal and the relative values across the series are shown.

Table S14. The relevant geometric parameters (for molecules around a reference molecule, satisfying the conditions, 2.5 < r' < 4.5 Å and r.sinα < 10 Å, and the relative rates of Dexter energy transfer in crystals of **1a-c**.

Crystal	r (Å)	r' (Å)	α (°)	δ (°)	r.sinα (Å)	S	$S.e^{-r'}$	Relative rate
1a	5.630	2.825	59.9	0.0	4.871	0.5017	0.0840	**1.000**
	5.630	2.825	59.9	0.0	4.871	0.5017	0.0840	
	3.929	3.515	26.5	0.0	1.756	0.8946	0.0934	
	8.052	4.206	58.5	0.0	6.866	0.5224	0.0328	
						Total	**0.2942**	
1b	7.737	2.645	70.0	38.4	7.271	0.2681	0.0190	**0.245**
	9.547	2.861	88.3	0.0	9.107	0.2997	0.0172	
	6.132	3.263	57.9	14.0	5.192	0.5163	0.0198	
	6.451	3.920	52.6	14.0	5.122	0.5895	0.0117	
	8.425	4.538	57.4	38.4	7.099	0.4224	0.0045	
						Total	**0.0722**	
1c	5.907	4.234	44.2	66.5	4.120	0.2858	0.0042	**0.014**
						Total	**0.0042**	

The relative rates of the two modes of energy transfer in crystals of **1a-c** are shown graphically in Fig. 6c of the main text.